Clean Techn Environ Policy (2011) 13:559–565
DOI 10.1007/s10098-011-0368-y

ORIGINAL PAPER

Numerical study of hydrogen production by the sorption-enhanced steam methane reforming process with online CO_2 capture as operated in fluidized bed reactors

Yuefa Wang · Zhongxi Chao · Hugo A. Jakobsen

Received: 11 November 2010 / Accepted: 4 March 2011 / Published online: 18 March 2011

Abstract A three-dimensional (3D) Eulerian two-fluid model with an in-house code was developed to simulate the gas-particle two-phase flow in the fluidized bed reactors. The CO_2 capture with Ca-based sorbents in the steam methane reforming (SMR) process was studied with such model combined with the reaction kinetics. The sorption-enhanced steam methane reforming (SE-SMR) process, i.e., the integration of the process of SMR and the adsorption of CO_2, was carried out in a bubbling fluidized bed reactor. The very high production of hydrogen in SE-SMR was obtained compared with the standard SMR process. The hydrogen molar fraction in gas phase was near the equilibrium. The breakthrough of the sorbent and the variation of the composition in the breakthrough period were studied. The effects of inlet gas superficial velocity and steam-to-carbon ratio (mass ratio of steam to methane in the inlet gas phase) on the reactions were studied. The simulated results are in agreement with the experimental results presented by Johnsen et al. (2006a, Chem Eng Sci 61:1195–1202).

Keywords Hydrogen production · CO_2 capture · SE-SMR · Fluidized bed · Numerical simulation

Y. Wang · Z. Chao · H. A. Jakobsen (✉)
Department of Chemical Engineering, Norwegian University of Science and Technology, NTNU, Sem Sælands vei 4, 7491 Trondheim, Norway
e-mail: hugo.atle.j@chemeng.ntnu.no

List of symbols

Variables

$C_{p,k}$	Specific heat capacity of phase k [J/(kg K)]
$C^{s}_{CO_2}$	CO_2 mass fraction in sorbent
d_p	Particle diameter [m]
D_{ji}	Binary diffusion coefficient [m^2/s]
$D_{k,j}$	Diffusion coefficient for component j in phase k [m^2/s]
H_i^R	Specific reaction enthalpy for reaction i (R = SMR, SP) [J/kg]
H_t	Height of reactor [m]
k	Rate coefficient
k_k	Thermal conductivity of phase k [W/(m K)]
K_1, K_2, K_3	Equilibrium constant
K_Y	Adsorption constants for component Y (Y = CH_4, CO_2, H_2, H_2O)
M	Molar mass [kg/kmol]
n	Reaction order of CO_2 adsorption
p	Pressure [Pa]
Q_k^i	Interfacial heat transfer to phase k [J/(m^3 s)]
r	Radius coordinate
R	Radius of reactor [m]
R_a	Adsorption rate of CO_2 in sorbent [kg/(kg s)]
R_i	Reaction rate of reaction i [kmol/(m^3 s)]
R_j	Formation rate of component j [kg/(m^3 s)]
r_{sc}	Mass ratio of steam to methane in the inlet gas phase
S	Specific surface area of sorbent [m^2/g]
Sh	Sherwod number
t	Time [s]
T	Temperature [K]
u_0	Inlet gas superficial velocity [m/s]
X	Conversion
y^{dry}	Dry molar fraction in gas phase

z	Axial coordinate
$\mathbf{b}$	Source vector
$\mathbf{C}_d$	Peculiar velocity [m/s]
$\mathbf{g}$	Gravity [m/s^2]
$\mathbf{M}_k$	Interfacial momentum transfer of phase k [N/m^3]
$\mathbf{r}_m$	Residual vector
$\tilde{v}'_c$	Fluctuating component of fluid velocity [m/s]
$\mathbf{v}_k$	Velocity of phase k [m/s]

Greeks

α_k	Volume fraction of phase k (k = c, d)
β	Interfacial drag coefficient [kg/(m^3 s)]
γ	Collisional energy dissipation [J/(m^3 s)]
ε	Convergence criterion
κ_d	Conductivity of granular temperature [kg/(m s)]
μ_k	Viscosity of phase k [kg/(m s)]
ρ_k	Density of phase k [kg/m^3]
τ_k	Stress tensor of phase k [N/m^2]
ω	Mass fraction
Γ	Averaged interfacial mass flux [kg/(m^3 s)]
Θ	Granular temperature [m^2/s^2]

Superscripts

dilute	Dilute
eff	Effective
i	Interfacial
k	Kinetic
SMR	Steam methane reforming
SP	CO_2 sorption by sorbent

Subscripts

a	Adsorption
c	Continuous phase
d	Dispersed phase, desorption
eq	Equilibrium
i	Reaction number
j	Component number
k	Phase (k = c, d)
p	Particle

Introduction

Hydrogen is an important material in the petroleum and chemical industries, and is considered to be a potential clean energy source. Hydrogen production from biomass is being studied by many authors (Bleeker et al. 2010; Elms and El-Halwagi 2010; Rivera-Tinoco and Bouallou 2010). However, hydrogen is still predominantly produced from fossil fuels, such as the steam methane reforming process (SMR) which produces hydrogen with by-product CO_2. With the increasing impact of global warming caused mostly by increasing concentrations of greenhouse gases, the emission control of CO_2 as the most important greenhouse gas was concerned by many researchers. The process of sorption-enhanced steam methane reforming (SE-SMR) is becoming an important topic due to its integration of hydrogen production and CO_2 separation. In this process, carbon dioxide is captured by an on-line sorbent, and the chemical equilibrium is shifted to the product side of the SMR reaction. Therefore, the higher hydrogen production may be obtained (Han and Harrison 1994). The sorbent with the adsorbed carbon dioxide can be regenerated using the temperature or pressure swing desorption to release the CO_2 for storage or other treatment. The SE-SMR reactions can proceed at temperatures of about 200°C lower than that for standard SMR process (Hufton et al. 1999). Amann et al. (2009) studied the CO_2 pre-combustion capture in a natural gas combined cycle power plant. De Castro et al. (2010) studied the hydrogen production by the auto-thermal reforming process coupled with the CO_2 capture and obtained 99% hydrogen products.

The experimental and theoretical studies on the SE-SMR process have been reported. The experimental results of CaO carbonation in a pilot-scale fluidized bed reactor by Abanades et al. (2004a, b) showed that high CO_2 capture efficiencies from combustion flue gas are obtained in a fluidized bed. Hughes et al. (2004) investigated cyclic carbonation and calcination reactions for CO_2 capture from combustion and gasification processes. Their approach may reduce the CO_2 emissions from coal- and petroleum coke-fired fluidized bed combustors by up to 85%. Johnsen et al. (2006a) conducted an experimental investigation on reforming and sorbent calcination in cyclic operation in a bubbling fluidized bed reactor. Wang et al. (2010) proposed a method for determination of the long-term sorbent activity and greatly reduced the experimental work for evaluation of hydrogen production and CaO-based CO_2 capture sorbent development.

Prasad and Elnashaie (2004) proposed a circulating fluidized bed membrane reactor for SMR with CO_2 sequestration using the CO_2-lime reaction and studied the reactor performance with a one-dimensional (1D) model. Johnsen et al. (2006b) modeled the SE-SMR and sorbent regeneration processes conducted continuously in two coupled bubbling beds with a homogeneous model. Li and Cai (2007) made a simulation of multiple cycles for SE-SMR and sorbent regeneration in a fixed bed reactor. Lindborg and Jakobsen (2009) studied the process performance and analyzed the reactor design for SE-SMR in a bubbling fluidized bed reactor using a two-dimensional (2D) model and pointed out that investigations of SE-SMR process using a three-dimensional (3D) multi-fluid model are needed.

A 3D two-fluid model was developed in this study. Moreover, an in-house program code for the numerical solution of the model has been written by the authors. The

performances of the SE-SMR process and the CaO sorbent in the fluidized bed reactors were studied using the developed 3D model implemented in the program code.

Numerical models

Hydrodynamic models

A 3D non-axisymmetric two-fluid model has been developed for the simulation of the SE-SMR process in fluidized bed reactors. The kinetic theory of granular flow and the k-ε turbulence model are used to describe the particle–particle interactions and the gas phase turbulence quantities, respectively. The drag model presented by Benyahia et al. (2006) is used in this work to account for the gas–solid interactions.

The governing equations for mass, momentum, species composition, and granular and molecular temperature are given in Table 1. More detailed descriptions of the model and solution methods can be found in Lindborg et al. (2007) and Lindborg and Jakobsen (2009).

Kinetic models

Xu and Froment (1989) presented a three-reaction model for SMR reactions:

$$CH_4 + H_2O \Leftrightarrow CO + 3H_2 \quad \Delta H_{298} = 206\ \text{kJ/mol} \tag{7}$$

$$CO + H_2O \Leftrightarrow CO_2 + H_2 \quad \Delta H_{298} = -41\ \text{kJ/mol} \tag{8}$$

$$CH_4 + 2H_2O \Leftrightarrow CO_2 + 4H_2 \quad \Delta H_{298} = 165\ \text{kJ/mol} \tag{9}$$

The kinetic equations for these reactions used in our simulations are:

$$R_1 = \frac{k_1}{p_{H_2}^{2.5}}\left[\frac{p_{CH_4}p_{H_2O} - p_{H_2}^3 p_{CO}\Big/K_1}{\text{DEN}^2}\right] \tag{10}$$

$$R_2 = \frac{k_2}{p_{H_2}}\left[\frac{p_{CO}p_{H_2O} - p_{H_2}p_{CO_2}/K_2}{\text{DEN}^2}\right] \tag{11}$$

$$R_3 = \frac{k_1}{p_{H_2}^{3.5}}\left[\frac{p_{CH_4}p_{H_2O}^2 - p_{H_2}^4 p_{CO_2}\Big/K_3}{\text{DEN}^2}\right] \tag{12}$$

where

$$\text{DEN} = 1 + K_{CO}p_{CO} + K_{H_2}p_{H_2} + K_{CH_4}p_{CH_4} + K_{H_2O}p_{H_2O}/p_{H_2} \tag{13}$$

The rate equation for CO_2 adsorption by the CaO sorbent is taken from Sun et al. (2008):

$$CaO + CO_2 \Leftrightarrow CaCO_3 \quad \Delta H_{298} = -178\ \text{kJ/mol} \tag{14}$$

$$R_a = \frac{dX}{dt} = 56k_s(1-X)\left(p_{CO_2} - p_{CO_2,eq}\right)^n S \tag{15}$$

Results and discussion

Hydrodynamic flow regimes

The catalytic SMR reactions and the CO_2 adsorption by sorbent take place simultaneously in a bubbling fluidized bed (BFB) reactor to provide sufficient residence time for the solid phase. The reactor is a cylinder of 4 m in length and 20 cm in diameter. The solid particles have diameter of 500 μm and density of 1,500 kg/m^3. The parameters used in the numerical simulation are listed in Table 2. The velocity profiles and the axial distribution of volume fraction of solid particles appear in Fig. 1. The velocity profiles display the heterogeneous structure of the bed and the non axial symmetric behavior of the solid flow. The axial distribution of solid phase is close to uniform.

Table 1 Governing equations

Continuity equation for phase k (=c, d):

$$\frac{\partial}{\partial t}(\alpha_k\rho_k) + \nabla\cdot(\alpha_k\rho_k\mathbf{v}_k) = 0 \tag{1}$$

Momentum equation for phase k (=c, d):

$$\frac{\partial}{\partial t}(\alpha_k\rho_k\mathbf{v}_k) + \nabla\cdot(\alpha_k\rho_k\mathbf{v}_k\mathbf{v}_k) = -\alpha_k\nabla p + \nabla\cdot\bar{\tau}_k + \alpha_k\rho_k\mathbf{g} + \mathbf{M}_k \tag{2}$$

Granular temperature equation:

$$\tfrac{3}{2}\left[\tfrac{\partial}{\partial t}(\alpha_d\rho_d\Theta) + \nabla\cdot(\alpha_d\rho_d\mathbf{v}_d\Theta)\right] = \bar{\tau}_d : \nabla\mathbf{v}_d + \nabla\cdot(\kappa_d\nabla\Theta) - \gamma - 3\beta\Theta + \beta\langle\mathbf{v}'_c\cdot\mathbf{C}_d\rangle + \tfrac{3}{2}\Gamma_k\Theta \tag{3}$$

Molecular temperature equation for phase c and d:

$$\alpha_c\rho_c C_{p,c}\frac{DT_c}{Dt} = \nabla\cdot\left(\alpha_c k_c^{\text{eff}}\nabla T_c\right) + \sum_i\left(-\Delta H_i^{\text{SMR}}\right)R_i^{\text{SMR}} + Q_c^i \tag{4}$$

$$\alpha_d\rho_d C_{p,d}\frac{DT_d}{Dt} = \nabla\cdot\left(\alpha_d k_d^{\text{eff}}\nabla T_d\right) + \left(-\Delta H^{\text{SP}}\right)R^{\text{SP}} - Q_c^i \tag{5}$$

Species composition:

$$\frac{\partial}{\partial t}\left(\alpha_c\rho_c\varpi_{c,j}\right) + \nabla\cdot\left(\alpha_c\rho_c\mathbf{v}_c\varpi_{c,j}\right) = \nabla\cdot\left(\alpha_c\rho_c D_{c,j}^{\text{eff}}\nabla\varpi_{c,j}\right) + M_j R_j^i \tag{6}$$

Table 2 List of numerical parameters

Particle diameter	500 μm
Particle density	1,500 kg/m^3
Sorbent-to-catalyst mass ratio	1:4
Reactor size	$R = 0.1$ m, $H_t = 4$ m
Initial bed height	2 m
Grid cell number	12 × 12 × 80
Time step	1×10^{-4} s
Convergence criterion	$\|\mathbf{r}_m\| < \varepsilon \|\mathbf{b}\| \quad \varepsilon = 10^{-10}$

Comparison between SE-SMR and standard SMR

Figures 2 and 3 display the outlet molar fraction of hydrogen, methane, and CO_2 in gas phase for the SMR and SE-SMR processes in the BFB reactor. In the SMR results, the outlet molar fraction of H_2 is only 75%, and a lot of CO_2 and CH_4 are emitted out of the reactor. However, in the simulations of the SE-SMR process, both the conversion of methane and the adsorption of CO_2 are larger than 99%. In this case, the amount of CO_2 produced in methane reforming reactions can be considered to be adsorbed totally by the sorbent, the methane reforming and hydrogen production are greatly enhanced. Figure 4 shows that the adsorption rate of CO_2 by sorbents is constant until $t = 210$ s. The sorbent capacity is large enough for the simulated conditions.

Sorbent capacity and breakthrough

The capacities of calcium-based sorbents (dolomite and limestone) are usually in the range of 0.3–0.6 g(CO_2)/g(sorbent) (Harrison 2008). On the basis of the results shown in Fig. 4, the carbonation rate of the sorbent is very slow under the simulation conditions. It may need much longer time to complete the carbonation of the sorbent. The simulations with smaller sorbent capacity were carried out. Figures 5 and 6 are the simulation results with the sorbent capacity of 0.05 g(CO_2)/g(sorbent).

Figure 5 shows the evolutions of CO_2 molar fraction in gas and mass fraction in solid phases during the SE-SMR process. When the CO_2 mass fraction in the solid phase was close to the sorbent capacity at the time of 12.5 min, the CO_2 molar fraction in gas phase began to increase rapidly, then reached a high level of about 0.15 mol/mol and been kept at this value later, which equals to the CO_2 fraction in the standard SMR process. The molar fractions of hydrogen and methane in gas phase also changed at the same time as shown in Fig. 6. The hydrogen fraction dropped to about 0.75 mol/mol, which is near the equilibrium of SMR. Three stages exist, two stable stages of pre-breakthrough and post-breakthrough, and one rapidly changed stage of breakthrough, which is similar to the experimental results of Han and Harrison (1994) and Johnsen et al. (2006a).

The rate of CO_2 capture by sorbent is almost constant in the pre-breakthrough as shown in Fig. 5. At this rate, the breakthrough of the real Ca-based sorbents with the capacity of 0.3–0.6 g(CO_2)/g(sorbent) may start at 75–125 min under the simulated conditions.

Effects of pressure and inlet gas superficial velocity on the reactions in SE-SMR

The above results show that the methane conversion and hydrogen production in the SE-SMR process greatly

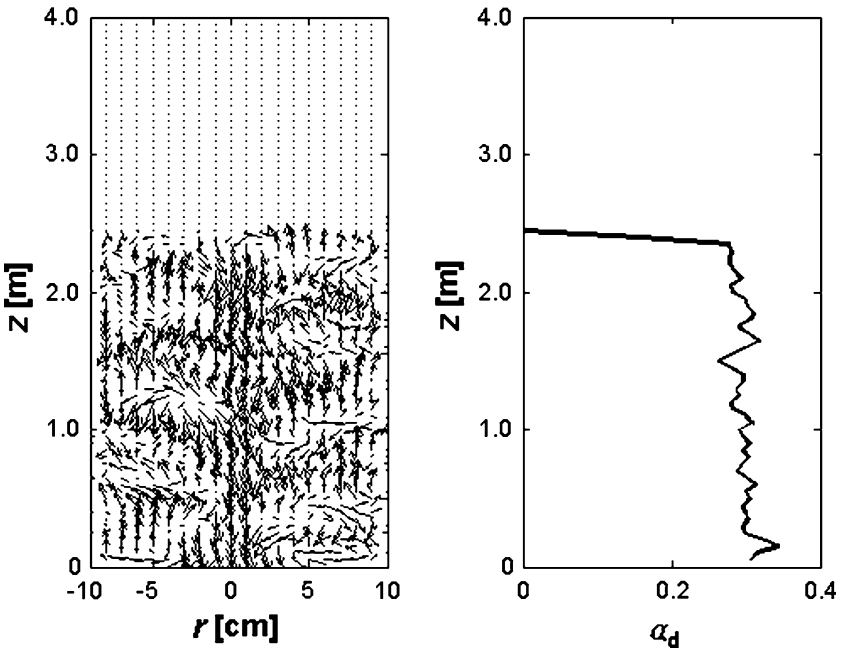

Fig. 1 Velocity profiles and volume fraction of solid particles in a bubbling fluidized bed reactor ($u_0 = 0.3$ m/s, $T = 848$ K, $r_{sc} = 5{:}1$, $p = 1$ bar)

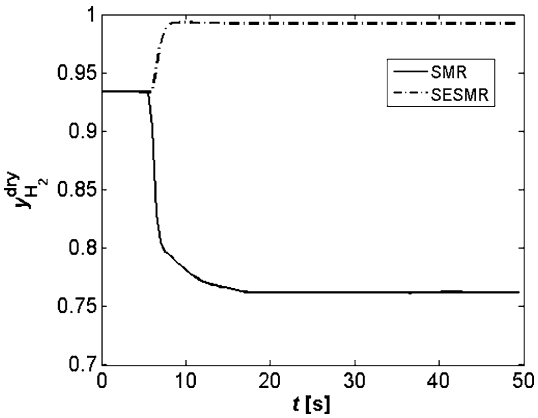

Fig. 2 Average outlet molar fraction of hydrogen for SMR and SE-SMR ($u_0 = 0.3$ m/s, $T = 848$ K, $r_{sc} = 5{:}1$, $p = 1$ bar)

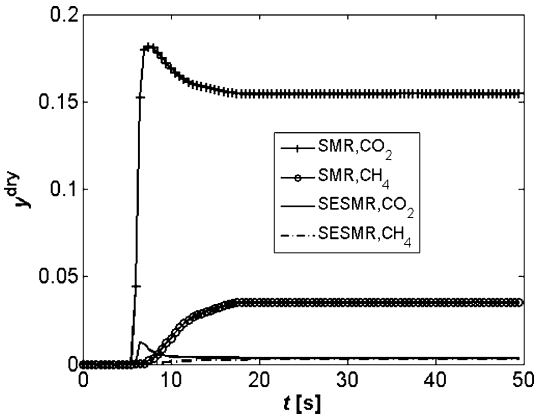

Fig. 3 Average outlet molar fraction of methane and CO_2 for SMR and SE-SMR ($u_0 = 0.3$ m/s, $T = 848$ K, $r_{sc} = 5{:}1$, $p = 1$ bar)

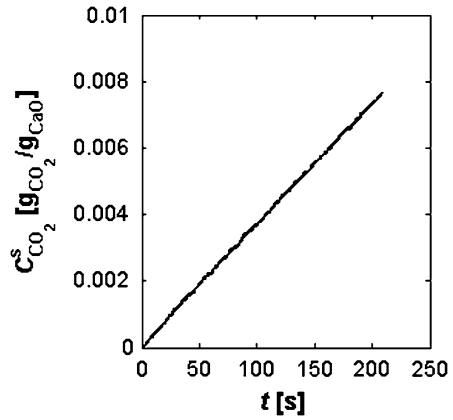

Fig. 4 Average mass fraction of CO_2 in sorbents for SE-SMR ($u_0 = 0.3$ m/s, $T = 848$ K, $r_{sc} = 5{:}1$, $p = 1$ bar)

depend on the rate of CO_2 removal by the sorbent and the sorbent capacity. When the sorbent capacity was fulfilled, the rate of CO_2 removal decreased rapidly to zero and the hydrogen molar fraction in gas phase dropped greatly. The

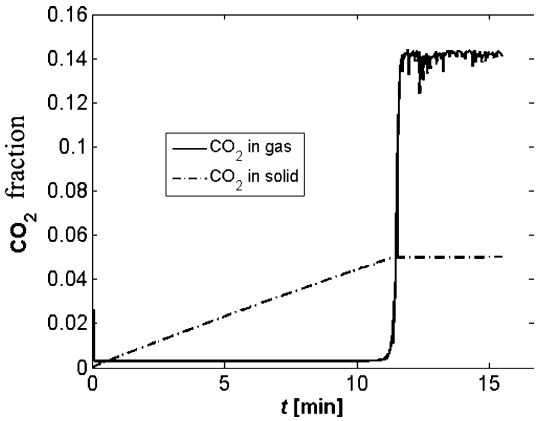

Fig. 5 The variation of CO_2 molar fraction in gas phase and mass fraction in solid phase with time ($u_0 = 0.89$ m/s, $T = 848$ K, $r_{sc} = 5{:}1$, $p = 1$ bar)

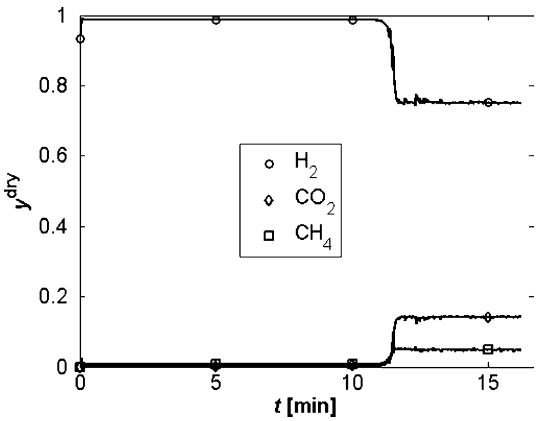

Fig. 6 The variation of methane, hydrogen, and CO_2 molar fractions in gas phase with time ($u_0 = 0.89$ m/s, $T = 848$ K, $r_{sc} = 5{:}1$, $p = 1$ bar)

influence of reactor pressure and the inlet gas superficial velocity are shown in Figs. 7 and 8.

Figure 7 shows that the adsorption rate of carbon dioxide by sorbents is higher at higher pressure. It is a natural result of the adsorption process. The CO_2 adsorption rate is increased as the gas superficial velocity increased (Fig. 8) and maintains constant with the time for the tested values of gas superficial velocity before the capacity of the sorbent was exhausted. The kinetic equation (15) for CO_2 adsorption shows that the reaction rate of CO_2 adsorption depends on the partial pressure of CO_2 and the specific surface area of sorbent. At the reactor startup and at lower superficial velocities, the SMR CO_2 production rate is relatively low, thus the partial pressure of CO_2 in the gas phase is low and only a fraction of the surface area of the sorbent is occupied by CO_2. Under these SMR conditions, the adsorption rate is low and far from its equilibrium. As a result, the adsorption rate will increase with the increase of partial pressure of CO_2 at the higher superficial velocities.

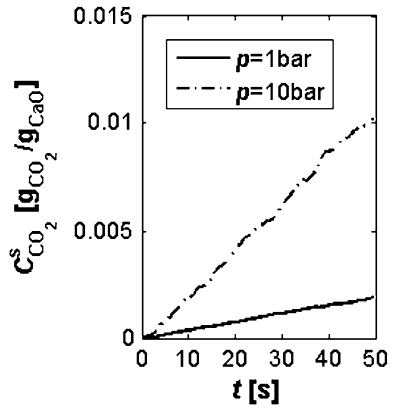

Fig. 7 Average mass fraction of CO_2 in sorbents at different pressures ($u_0 = 0.3$ m/s, $T = 848$ K, $r_{sc} = 5{:}1$)

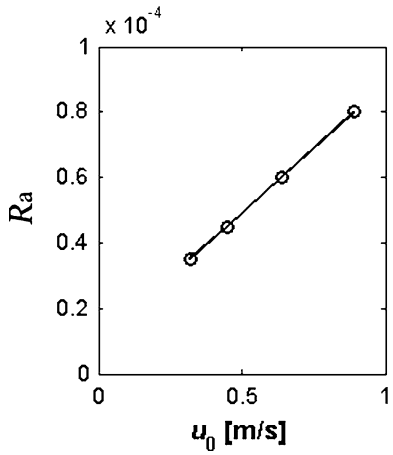

Fig. 8 Average adsorption rate of CO_2 at different inlet gas superficial velocities ($T = 848$ K, $r_{sc} = 5{:}1$, $p = 1$ bar)

Abanades et al. (2004a, b) reported high CO_2 capture efficiencies by CaO were obtained for flue gases at superficial velocity of 1 m/s. The maximum gas superficial velocity in our simulations is 0.89 m/s, which is close to their results but still lower than that one. Figure 9 shows that the hydrogen fraction in gas phase is near equilibrium for SE-SMR process before the sorbent breakthrough at the gas superficial velocity of up to 0.89 m/s. The time for breakthrough decreased with the increase of the gas superficial velocity. It is in agreement with the experimental results of Johnsen et al. (2006a).

Effects of steam-to-carbon ratio

Increasing steam-to-carbon ratio results in increasing of hydrogen production as shown in Fig. 10. The outlet hydrogen molar fraction in gas phase increases from 0.9614 to 0.9881 as the steam-to-carbon ratio increases from 3 to 4. Increased hydrogen molar fraction in gas phase

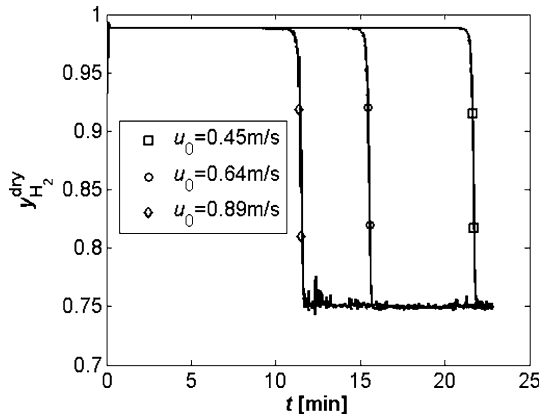

Fig. 9 The variation of hydrogen molar fraction in gas phase with time ($T = 848$ K, $r_{sc} = 5{:}1$, $p = 1$ bar)

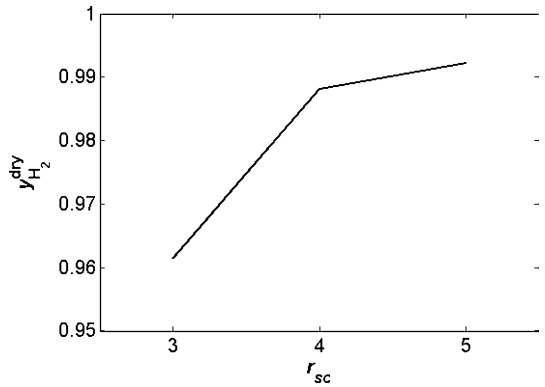

Fig. 10 Hydrogen molar fraction in gas phase under different steam-to-carbon ratios ($p = 1$ bar, $u_0 = 0.3$ m/s, $T = 848$ K)

is 2.78%. While the hydrogen molar fraction in gas phase increases only 0.415% (from 0.9881 to 0.9922) as the steam-to-carbon ratio increases from 4 to 5. The range of steam-to-carbon ratio from 3 to 4 is a better choice for SE-SMR process as proposed by Johnsen et al. (2006b). After the steam-to-carbon ratio exceeds 4, the steam consumption will increase greatly with only a little increase of hydrogen production.

Conclusion

The simulation results show that the integration of CO_2 sorption into the SMR process can enhance the methane conversion to hydrogen greatly. Higher hydrogen production near equilibrium was obtained in the bubbling fluidized bed reactor. The adsorption rate of CO_2 by the CaO sorbent is fast enough compared with the SMR rate. The sorbent can completely adsorb the CO_2 produced in the SE-SMR process at the gas superficial velocity up to 0.89 m/s for a long time. The adsorption rate of CO_2 is

higher at higher gas superficial velocity and higher pressure. The best value of steam-to-carbon ratio is about 4 in considering the balance between higher hydrogen production and the lower steam consumption.

Three stages about the sorbent breakthrough were obtained. Pre-breakthrough and post-breakthrough stages are stable, breakthrough stage is changed rapidly. The time for breakthrough decreased with the increase of gas superficial velocities. The simulated results are in agreement with the experimental results reported in the literatures (Han and Harrison 1994 and Johnsen et al., 2006a).

Desorption of CO_2 from the carbonated sorbent is a necessary additional process for the SE-SMR process to operate properly. The desorption apparatus will thus increase the total costs and the energy consumption of the process plant. On the other side, the heat released by the adsorption of CO_2 may compensate for some of the energy consumed in the desorption process. Furthermore, the introduction of CO_2 adsorption increased the methane conversion to near 100%. Hence, the cost for circulation of un-reacted materials can be saved. Therefore, the increased plant cost may be associated with the apparatus for desorption only. Of course, the main purpose of reducing the emission of CO_2 to the air was achieved.

Acknowledgments The post doc fellowship (Wang, Y.) financed through the RENERGI program (Hydrogen Production by Sorbent Enhanced Reforming) of the Norwegian Research Council and the PhD fellowship (Chao, Z.) financed through the GASSMAKS program (Advanced Reactor Modeling and Simulation) are gratefully appreciated.

References

Abanades JC, Anthony EJ, Lu DY, Salvador C, Alvarez D (2004a) Capture of CO_2 from combustion gases in a fluidized bed of CaO. AIChE J 50:1614–1622

Abanades JC, Rubin ES, Anthony EJ (2004b) Sorbent cost and performance in CO_2 capture systems. Ind Eng Chem Res 43: 3462–3466

Amann JM, Kanniche M, Bouallou C (2009) Reforming natural gas for CO_2 pre-combustion capture in combined cycle power plant. Clean Technol Environ Policy 11:67–76

Benyahia S, Syamlal M, O'Brien TJ (2006) Extension of Hill-Koch-Ladd drag correlation over all ranges of Reynolds number and solids volume fraction. Powder Technol 162:166–174

Bleeker M, Gorter S, Kersten S, van der Ham L, van der Berg H, Veringa H (2010) Hydrogen production from pyrolysis oil using the steam-iron process: a process design study. Clean Technol Environ Policy 12:125–135

De Castro J, Rivera-Tinoco R, Bouallou C (2010) Hydrogen production from natural gas: auto-thermal reforming and CO_2 capture. Chem Eng Trans 21:163–168

Elms RD, El-Halwagi MM (2010) The effect of greenhouse gas policy on the design and scheduling of biodiesel plant with multiple feedstocks. Clean Technol Environ Policy 12:547–560

Han C, Harrison DP (1994) Simultaneous shift reaction and carbon dioxide separation for the direct production of hydrogen. Chem Eng Sci 49:5875–5883

Harrison DP (2008) Sorption-enhanced hydrogen production: a review. Ind Eng Chem Res 47:6486–6501

Hufton JR, Mayorga S, Sircar S (1999) Sorption enhanced process for hydrogen production. AIChE J 45:248–256

Hughes RW, Lu D, Anthony EJ, Wu Y (2004) Improved long-term conversion of limestone derived sorbents for in situ capture of CO_2 in a fluidized bed combustor. Ind Eng Chem Res 43:5529–5539

Johnsen K, Ryu HJ, Grace JR, Lim CJ (2006a) Sorption-enhanced steam reforming of methane in a fluidized bed reactor with dolomite as CO_2-acceptor. Chem Eng Sci 61:1195–1202

Johnsen K, Grace JR, Elnashaie S, Kolbeinsen L, Eriksen D (2006b) Modeling of sorption-enhanced steam reforming in a dual fluidized bubbling bed reactor. Ind Eng Chem Res 45:4133–4144

Li Z, Cai N (2007) Modeling of multiple cycles for sorption-enhances steam methane reforming and sorbent regeneration in fixed bed reactor. Energy Fuels 21:2909–2918

Lindborg H, Jakobsen HA (2009) Sorption enhanced steam methane reforming process performance and bubbling fluidized bed reactor design analysis by use of a two-fluid model. Ind Eng Chem Res 48:1332–1342

Lindborg H, Lysberg M, Jakobsen HA (2007) Practical validation of the two-fluid model applied to dense gas-solid flows in fluidized beds. Chem Eng Sci 62:5854–5869

Prasad P, Elnashaie SSEH (2004) Novel circulating fluidized-bed membrane reformer using carbon dioxide sequestration. Ind Eng Chem Res 43:494–501

Rivera-Tinoco R, Bouallou C (2010) Using biomass as an energy source with low CO_2 emissions. Clean Technol Environ Policy 12:171–175

Sun P, Grace JR, Lim CJ, Anthony EJ (2008) Determination of intrinsic rate constants of the CaO-CO_2 reaction. Chem Eng Sci 63:47–56

Wang J, Manovic V, Wu Y, Anthony EJ (2010) CaO-based sorbents for capturing CO_2 in clean energy processes. Chem Eng Trans 21:187–192

Xu J, Froment GF (1989) Methane steam reforming, methanation and water-gas shift: I. Intrinsic kinetics. AIChE J 35:88–96